MODELING ACTIVITIES ON CAVITATING FLOWS AT CENTROSPAZIO

Emilio Rapposelli[**] and Luca d'Agostino[*]

Centrospazio – Consorzio Pisa Ricerche, 56121 Ospedaletto, Pisa, Italy

Abstract

The present paper illustrates recent theoretical and numerical activities on cavitating flows carried out at CENTROSPAZIO in the last few years. Specifically, it deals with the development and application of a modified isenthalpic cavitation model that accounts in an approximate but physical way for the occurrence of thermal cavitation effects and the concentration of active cavitation nuclei in the liquid. Expanding on the work of Brennen (1994), the model leads to a quasi-homogeneous barotropic description of cavitating flows, whose sound speed smoothly reduces to that of the liquid in the limit for low void fractions, thus eliminating the inconsistencies of previous formulations. Thermal effects are accounted for by assigning a single parameter expressing the nondimensional thickness of the thermal boundary layer in the liquid surrounding the growing cavities. The value of this parameter is related to the concentration of active cavitation nuclei, whose value can therefore be alternatively used to specify the impact of thermal cavitation effects. Applications to cavitating journal bearings, hydrofoils and helical inducers relevant to space engineering are presented.

Nomenclature

Latin Symbols

a	sound speed
b	bubble semi-separation
c	chord
C	bearing clearance
C_p	pressure coefficient
e	eccentricity
f	nondimensional impeller force
$\mathbf{F}$	nondimensional bearing force
H	height of the lubricating film
i	imaginary unit
K_C	cavitation parameter
L	bearing length
M	Mach number
m	mass
$\dot{m}$	mass flow rate
n	no. of active nuclei per unit liquid volume
N_B	number of blades
N_R	number of blade revolutions
p	pressure
P	blade axial pitch
Q_{vap}	heat of vaporization
r	radial coordinate
Re	Reynolds number
T	temperature
$\boldsymbol{u}$	velocity vector
V	volume
X_g	noncondensable gas fraction
x, y	lateral coordinates
z	axial coordinate

Greek Symbols

α	volume fraction, void fraction
α_T	thermal diffusivity
β	blade angle
δ	cavitation layer thickness
δ_T	thermal boundary layer thickness
ε	volume fraction, relative eccentricity
ϑ	azimuthal coordinate, angle of attack
ζ	nondimensional damping coefficient
μ	Newtonian viscosity
ν	kinematic viscosity
ρ	density
σ	Euler cavitation number
φ	velocity potential
ω	rotational speed
Ω	whirl speed

Subscripts

C	cavitation
H	hub
L	liquid
R	radial
sat	saturation
T	tip, tangential
V	vapor

Introduction

Cavitation is the major source of degradation of the suction performance, reliability, power density and useful life of liquid rocket propellant turbopumps, and the cause of other equally undesirable effects such as the reduction of the overall efficiency and the drastic increase of the noise generation (Stripling & Acosta, 1962). Even more importantly for space applications, cavitation can provide the necessary flow excitation, compliance and load-dependence for triggering dangerous rotordynamic and/or fluid mechanic instabilities of the turbopump (Sack & Nottage, 1965; Natanzon et al., 1974; Brennen & Acosta, 1973, 1976; Ng & Brennen, 1978; Braisted & Brennen, 1980; d'Auria, d'Agostino & Brennen, 1994, 1995; d'Agostino & d'Auria 1997; d'Agostino & Venturini-Autieri 2002), or even, through the coupling with thrust generation, of the entire propulsion system (POGO auto-oscillations of liquid propellant rockets, Rubin, 1966).

[**] Research Engineer, Centrospazio – Consorzio Pisa Ricerche, 5 Via A. Gherardesca, 56121 Ospedaletto (Pisa), Italy; e.rapposelli@cpr.it.

[*] Professor, Department of Aerospace Engineering, Via G. Caruso, 56126 Pisa, Italy; luca.dagostino@ing.unipi.it.

The recent fatigue failure of an inducer blade due to cavitation-induced fluid dynamic instabilities of the LE-7 liquid Hydrogen turbopump (NASDA Report No. 94, May 2000, NASDA Report No. 96, June 2000) and, more generally, supersynchronous and subsynchronous shaft vibrations experienced in the Space Shuttle main engine and in the Ariane 5 engine turbopumps (Ryan et al. 1994; Goirand et al. 1992; Kamijo, Yoshida & Tsujimoto 1993) dramatically confirmed that the combined effects of cavitation and rotordynamic fluid forces represent the dominant fluid mechanical phenomena that adversely affect the dynamic stability and pumping performance of high power density turbopumps (Brennen, 1994). The most critical rotordynamic instability in turbopumps is the development of self-sustained lateral motions of the impeller under the action of destabilizing forces of mechanical or of fluid dynamic origin. Because of their greater complexity, rotordynamic fluid forces have so far received relatively little attention in the open literature, despite of their well recognized potential for promoting rotordynamic instabilities of high performance turbopumps (Rosenmann 1965) and for significantly modifying, in conjunction with cavitation, the dynamic properties of the impeller, and therefore the critical speeds of the whole machine (Jery et al. 1985; Franz 1989; Bhattacharyya 1994; d'Auria, d'Agostino & Brennen 1995; d'Agostino & d'Auria 1997; d'Agostino, d'Auria & Brennen 1998; d'Agostino & Venturini-Autieri 2002; Rapposelli, Falorni & d'Agostino 2002). Available evidence clearly indicates that the current trend towards supercritical operation of turbopumps for liquid propellant feed systems imposes careful reconsideration of the contributions of rotordynamic fluid forces on cavitating impellers in determining the dynamic properties of the rotors. Simple overestimation of these forces with reference to noncavitating operation is just not acceptable in supercritical machines since it would lead to unrealistically low values of the critical speeds and to drastic overestimates of the stability margins at design conditions, where significant cavitation is usually accepted.

Cavitation or ventilation of the lubricating fluid are frequently experienced also in journal bearings and squeeze-film dampers, where they significantly reduce the magnitude of bearing forces and modify their orientation with respect to the fully-wetted flow case (Dowson and Taylor, 1975; Swales, 1975). Future high power density rocket engine turbopumps with propellant lubricated hydrodynamic bearings are particularly critical in this respect because the relatively high saturation pressure and low viscosity of most propellants promote bearing cavitation and operation at larger eccentricity and Reynolds numbers, where the inertia of the lubricant and thermal cavitation effects become significant, enhancing the danger of rotordynamic instabilities.

Because of the articulation and complexity of the phenomena involved, cavitating flows cannot be accurately predicted by analytical methods. The development and validation of workable engineering models for numerical simulation of cavitating flow represent therefore natural and important steps for progress in this field.

Cavitation Model

A major difficulty in the analysis of cavitating flows is the presence of free surfaces, whose shape, location and evolution are not known "a priori" and must in principle be obtained as part of the solution of the flow field. Cavitating flows are therefore intrinsically unsteady on a length scale comparable to the cavity size and often also on the global (macroscopic) scale, especially in internal reverberating flows. Therefore cavitation poses formidable obstacles in terms of both physical and numerical modeling. Successful development of a model for simulating cavitation in technical applications must be based on careful consideration of the final objectives and implementation constraints, in order to exploit all opportunities to simplify the formulation of the problem by including only the essential physical phenomena. Specifically, the typical requirements of space propulsion applications to the analysis of propellant feed turbopumps put especial prize on the suction and dynamic performance of the machine rather than on its resistance to erosion and other long-term effects of cavitation, which are typically a major concern in other applications. Moreover, typical propellants for space launchers are cryogenic fluids stored close to saturation conditions. In these fluids thermodynamic phenomena are known to represent the dominant source of cavitation scaling effects due to the temperature difference between the two phases that develops as a consequence of the volume changes of the cavities. In turn, this temperature difference modifies the vapor pressure in the cavities with respect to the unperturbed value corresponding to the bulk temperature of the liquid, thereby significantly affecting the pressure differential that ultimately drives the dynamic response of the cavities. Effective flow models for accurate simulation of cavitating flows in space propulsion applications must therefore account for thermal cavitation effects.

Considering that adiabatic force-free flows of cavitating liquids are practically isenthalpic and that the thermal term dominates the kinetic, viscous and unsteady contributions in the enthalpy equation, it is possible to use the energy balance of the mixture to relate density (or, equivalently, the void fraction) to the local value of the pressure. In this approximation therefore the flow is barotropic, which represents a significant advantage of the isenthalpic formulation, as it reduces the order of the differential problem governing the flow field. Using these considerations, a quasi-homogeneous bubbly liquid/vapor model, suitably modified to account for thermal effects (Rapposelli and d'Agostino,

2001) has been developed and used to describe the occurrence of flow cavitation in several numerical and analytical analyses. The proposed model treats the fully-wetted and two-phase portions of the fluid in a unified manner in order to avoid the use of "ad hoc" matching conditions, whose applicability and accuracy is questionable in flows where significant inertial and/or unsteady effects are present, a situation that is likely to occur in turbopumps for space applications. After careful consideration, this model seemed to offer the best compromise between physical consistency, ease of implementation and accuracy in the application to the performance prediction of cavitating turbomachinery for liquid propellant rocket fuel feed systems.

The cavitation model has been presented in detail in previous papers (Rapposelli and d'Agostino, 2001). Here we just outline the main steps of its derivation. Considering that for a given mass $m = \rho V$ of the cavitating mixture subject to a pressure change dp, it is possible to derive the following expression of the sound speed:

$$\frac{1}{\rho a^2} = \frac{1}{\rho}\frac{d\rho}{dp} = \frac{\alpha_L}{\rho_L}\left(\frac{d\rho_L}{dp}\right) + \frac{\alpha_V}{\rho_V}\left(\frac{d\rho_V}{dp}\right) + \left(\frac{1}{\rho_L} - \frac{1}{\rho_V}\right)\frac{\rho}{m}\frac{dm}{dp}$$

where $\alpha_V = 1 - \alpha_L$ is the void fraction and dm is the mass exchange between the two phases. In this expression the conditions for the evaluation of the density derivatives depend on the heat exchanges between the two phases and must be specified. The two classical limit cases are the *frozen flow model*, where no heat and mass exchanges are assumed to occur, and the *equilibrium flow model*, where the two phases are assumed to be at thermal and mass diffusion equilibrium. In real cavitating flow the two phases are finitely dispersed and their thermal contact is only partial. Therefore the frozen flow and equilibrium approximations are relatively inaccurate, since they either neglect or overestimate the occurrence of thermal cavitation effects. A more realistic representation is obtained if it is assumed that thermodynamic equilibrium is only established with fraction $0 \le \varepsilon_L \le 1$ and $0 \le \varepsilon_V \le 1$ of the total volume of the liquid and vapor phases:

$$V = (1-\varepsilon_L)V_L + \varepsilon_L V_L + (1-\varepsilon_V)V_V + \varepsilon_V V_V$$

In these assumptions it is possible to show that:

$$\frac{1}{\rho a^2} = \frac{1-\alpha}{p}\left[(1-\varepsilon_L)f_L + \varepsilon_L g_L\right] + \frac{\alpha}{p}\left[(1-\varepsilon_V)f_V + \varepsilon_V g_V\right]$$

where $\alpha = \alpha_V = 1 - \alpha_L$ is the void fraction and f_L, g_L, f_V, g_V are known functions of the pressure and of the thermophysical properties of the two phases. Since both $f_V \cong g_V$, the influence of ε_V is negligible and only ε_L is practically relevant. In particular, for bubbly cavitating flows ($\alpha < 1$) the value of ε_L can be readily estimated in terms of the characteristic values of the bubble radius, R, the bubble separation, b, and the thickness, δ_T, of the thermal boundary layer in the liquid surrounding the bubble interface. As will be shown later, the ratio δ_T / R is approximately constant during the growth of thermally controlled vapor cavities. In these assumptions $\alpha \approx R^3 / b^3$ and:

$$\varepsilon_L \cong \frac{(R+\delta_T)^3 - R^3}{b^3 - R^3} = \frac{R^3}{b^3 - R^3}\left[\left(1 + \frac{\delta_T}{R}\right)^3 - 1\right] = \frac{\alpha}{1-\alpha} B \le 1 \qquad \text{where} \qquad B \approx \left[\left(1 + \frac{\delta_T}{R}\right)^3 - 1\right]$$

Clearly ε_L must level up to unity for any given value of δ_T / R as $\alpha \to 1$ and the above expression is only valid for void fractions not exceeding the value corresponding to $\varepsilon_L = 1$. Hence, with a minor approximation, ε_L is taken equal to the λ-th order harmonic mean:

$$\varepsilon_L = \left[\left(\frac{\alpha}{1-\alpha} B\right)^{-\lambda} + 1\right]^{-1/\lambda}$$

of the limit expressions of ε_L for low and high void fractions. In this equation, consistently with the present model, it can be shown that $\lambda \cong 3$ for the overlap of the thermal boundary layers of neighboring bubbles to occur for a radius change $\Delta R \approx \delta_T$. This formulation provides a smooth transition between the two expressions of ε_L, as expected in real flows as a consequence of the gradual overlapping of the thermal boundary layers.

In the thermally-controlled growth of a cavitating spherical bubble $\delta_T \cong \sqrt{\alpha_{TL} t}$ and $R \cong R^* \sqrt{t}$, where α_{TL} is the thermal diffusivity of the liquid. Therefore δ_T / R is approximately constant and can be considered as a free parameter, which determines the value of ε_L and accounts for the influence of thermal cavitation effects. Clearly δ_T / R ranges from zero in frozen flows to $\delta_T / R >> 1$ in isothermal equilibrium flows.

The value of $\delta_T / R \cong \sqrt{\alpha_{TL}} / R^*$ can also be estimated from the expression of $R^* = \left(-C_{p_{\min}} - \sigma\right) U_o^2 / \Sigma(T)$ (Brennen 1995) as a function of the reference flow velocity U_o, the cavitation number $\sigma = (p_o - p_{\text{sat}}) / \frac{1}{2}\rho_L U_o^2$, the local pressure coefficient $C_p \cong C_{p_{\min}}$, and the thermodynamic parameter $\Sigma(T) = \rho_{\text{sat}}^2 Q_{\text{vap}}^2 / \rho_L^2 c_{pL} T \sqrt{\alpha_{TL}}$, which depends on the latent

heat of vaporization $Q_{\text{vap}} = h_V - h_L$, the saturation conditions of each fluid, and is a strong function of the temperature T. However, the value of R^* for a single bubble is clearly overestimated, since the presence of multiple bubbles reduces their growth rate. In the present approximation, from the combined-phase continuity and momentum equations of the mixture it follows that two cavitating flows (indexes 1 and 2) with the same boundary conditions have equal velocity and pressure fields if $\alpha_1 = \alpha_2$. Therefore, since $nR^3 \cong \alpha/(1-\alpha)$ where n is the number of active cavitation nuclei per unit liquid volume, it follows that:

$$\frac{R_2^*}{R_1^*} = \frac{R_2}{R_1} = \left[\frac{n_1\alpha_2(1-\alpha_1)}{n_2\alpha_1(1-\alpha_2)}\right]^{1/3} = \left(\frac{n_1}{n_2}\right)^{1/3}$$

For the flow with a single bubble $n_1 \cong 1/V_C$, where V_C is the cavitation volume ($p \le p_{\text{sat}}$) of the flow. Corrected values of $\delta_T/R \cong \sqrt{\alpha_{TL}}/R_2^*$ for cavitation in waters near room conditions with typical values of the concentrations of active nuclei (10 to $100\ \text{cm}^{-3}$) are consistent with the estimates of δ_T/R obtained by fitting numerical simulations of the cavitating flow with the available experimental data. Extrapolation to higher temperatures is more uncertain, presumably because of the temperature dependence of the active nuclei concentration.

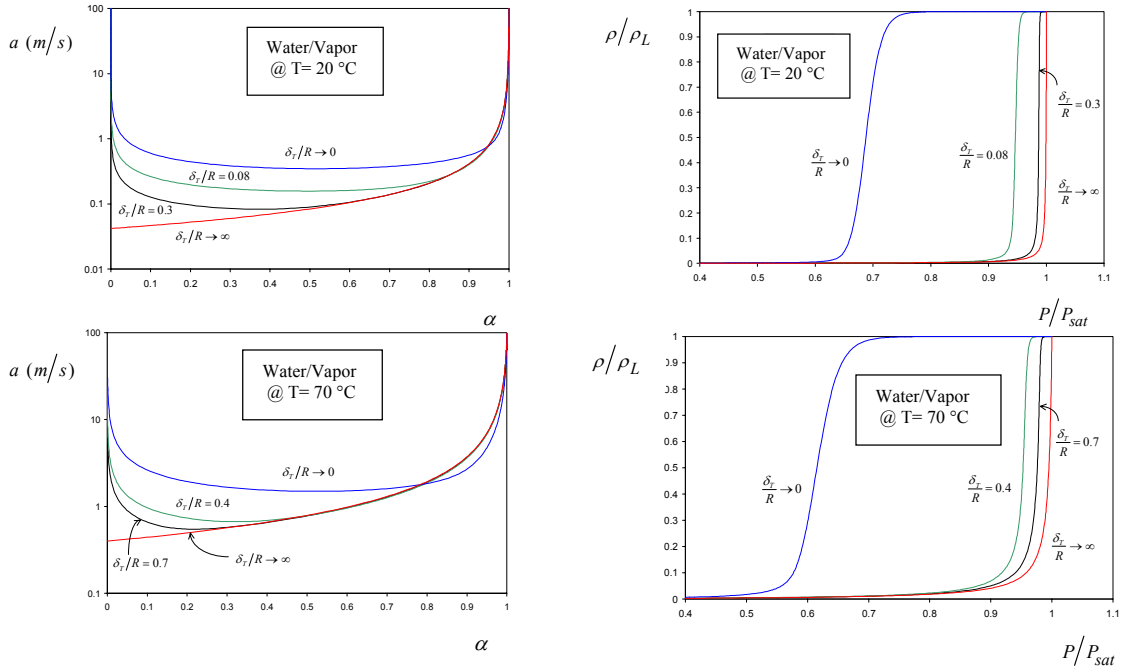

Figure 1. Sonic velocities as functions of the void fraction α and barotropic curves as functions of the pressure p/p_{sat} for bubbly water/vapor mixtures at 20 °C and 70°C and several values of δ_T/R.

Figure 1 shows the barotropic law and the sound speed of a liquid/vapor mixture as functions of the void fraction for water at 20 and 70 °C for several values of δ_T/R. Values of δ_T/R between 0.3 and 0.7 have been found to be the most realistic by comparing numerical simulations with experimental data and have been used in the following calculations. Figure 1 shows that the sound speed drops by several orders of magnitude to extremely low values even for moderate void fractions. It follows that in cavitating flows both nearly incompressible zones (pure liquid) and regions where the flow may easily become highly supersonic (liquid-vapor mixtures) are present and need to be solved simultaneously. The resulting stiffness of the numerical problem is further increased both by the high density ratio between the two phases (for water at 20 °C the liquid-to-vapor density ratio is on the order of 10^5) and by the strong shock discontinuities occurring in the recondensation at the cavity closure. This singular behavior reflects the large variations of the sound speed with the pressure as the flow transitions from a fully-wetted liquid to a two-phase cavitating mixture. For instance, in the above example the speed of sound of water at room temperature is about 1500 m/s, 400 m/s ca. for pure vapor, and as low as a fraction of a m/s for a water-vapor mixtures at intermediate values of the void fraction.

After careful consideration, this model has been chosen as the best compromise between physical consistency, ease of implementation and accuracy in the application to the performance prediction of cavitating turbomachinery for liquid

propellant rocket fuel feed systems. After careful consideration, this model has been conceived as the best compromise between physical consistency, ease of implementation and accuracy in the application to the performance prediction of cavitating turbomachinery for liquid propellant rocket fuel feed systems.

Cavitating Inducers

This section investigates the linearized dynamics of the three-dimensional flow in finite-length helical inducers with attached blade cavitation, with the purpose of understanding the impact of the cavitation response on the rotordynamic forces exerted by the fluid on the impeller of whirling turbopumps. The available experimental evidence indicates that cavitation reduces the magnitude of the rotordynamic fluid forces, significantly affecting the added mass of the rotor. It is worth nothing that the consequent increase of the critical speeds is of special relevance to highly-loaded supercritical machines, as commonly used in liquid propellant rocket feed systems. A second major effect of cavitation is the introduction of a complex oscillatory dependence of the rotordynamic fluid forces on the whirl frequency. This finding seems to indicate the possible occurrence of resonance phenomena in the compressible cavitating flow inside the blade channels under the excitation imposed by the eccentric motion of the rotor. Earlier theoretical analyses have addressed the case of infinitely-long whirling helical inducers with uniformly distributed travelling bubble cavitation (d'Auria et al., 1995; d'Agostino and d'Auria, 1997; d'Agostino, d'Auria and Brennen 1998). The results confirmed the presence of internal flow resonances and indicate that bubble dynamic effects do not play a major role, except, perhaps, at extremely high whirl speeds. They also suggest that the assumptions of uniformly-distributed bubbly cavitation and infinitely long inducers may contribute to explain the discrepancies between theoretical predictions and experimental data. Following up on this work, the dynamics of the unsteady three-dimensional flow in finite-length helical inducers with attached blade cavitation has been investigated.

The linearized governing equations for the complex velocity perturbation $\tilde{\varphi}$ in a cavitating helical inducer rotating at constant angular speed ω and whirling about the stator axis with constant eccentricity e and angular speed Ω are:

$$\nabla^2\tilde{\varphi} = 0 \qquad \text{and} \qquad \frac{\partial'\tilde{\varphi}}{\partial t} + \overline{\boldsymbol{u}}' \cdot \nabla\tilde{\varphi} + \frac{\tilde{p}}{\rho_L} = 0$$

where $\overline{\boldsymbol{u}}'$ is the unperturbed flow velocity in the rotating frame, and $\tilde{p}$ is the complex amplitude of the pressure perturbation. These equations have been complemented with the appropriate boundary conditions and solved by separation of variables. Thin blades with constant hub and tip radii, r_H and r_T, are assumed, as schematically illustrated in Figure 2. Cavitation is thought to occur on the suction sides of the blades in the form of slowly-moving attached pockets uniformly distributed in a thin layer of given thickness $\delta << P$ and damped acoustic admittance $\rho_C a_C^2(1+i\zeta)$, where ζ is the nondimensional damping coefficient. The values of the (real) acoustic admittance $\rho_C a_C^2$ have been obtained from the isenthalpic cavitation model by making reasonable estimates of the void fraction, and appear in the model through the parameter describing the behaviour of the cavitating layer:

$$K_C = \frac{\rho_l \delta P^*}{\rho_C a_C^2(1+i\zeta)}$$

where $P^* = (P/N_B)\cos\beta$ is the width of the blade channels.

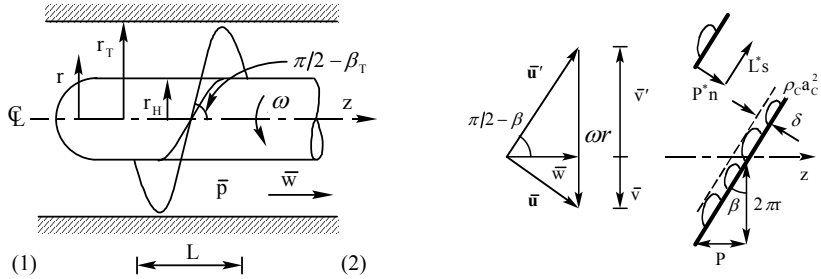

Figure 2. Schematic of the flow configuration, the inducer geometry (left) and the thin layer of attached cavitation pockets on the suction sides of the inducer blades (right).

In spite of the simplifications introduced in order to obtain an efficient closed form solution, comparison with the available experimental data indicates that the these theories correctly predict some of the observed features of the rotordynamic fluid forces in cavitating inducers. The results confirmed the presence of internal flow resonances and indicate that bubble dynamic effects do not play a major role, except, perhaps, at extremely high whirl speeds. The

influence of the cavitation parameter on the solution is illustrated by the waterfall plots of Figure 3. The figure clearly shows that the degree of cavitation, increasing with the value of $\mathrm{Re}\{K_C\omega^2\}$, has a major impact in locating the critical speeds and determining the magnitude of the rotordynamic forces as functions of the whirl speed. Two sets of symmetrically subsynchronous/supersynchronous resonances are predicted. At higher values of the cavitation parameter the amplitudes of the resonances decrease, as their frequencies approach synchronous conditions. Unstable frequency components with these properties have actually been observed in the vibration spectra of the SSME turbopumps (Zoladz, 2002) under cavitating conditions.

These investigations of rotordynamic forces in whirling and cavitating inducers represents the first theoretical analyses on this subject and yielded very significant results, clearly showing that the behavior of lateral whirl forces is strictly connected with the two-phase nature of the flow and providing useful practical indications and fundamental understanding of its dependence on the relevant flow conditions and parameters.

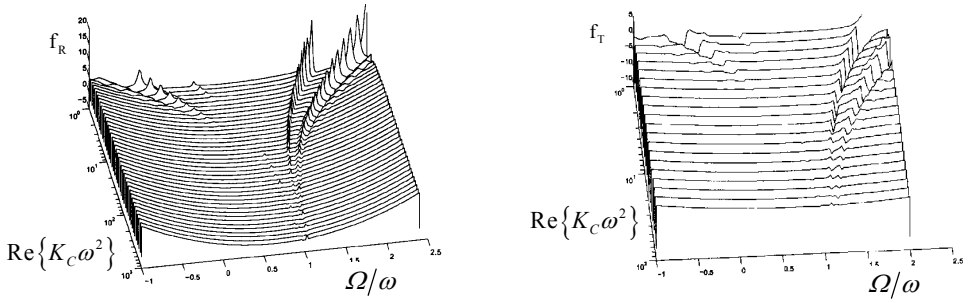

Figure 3. Waterfall plots of the nondimensional rotordynamic forces f_R, f_T on the test inducer as a function of the ratio Ω/ω of the whirl and rotational speeds and the real part of the nondimensional cavitation parameter, $K_C\omega^2$. The flow coefficient is $\phi = 0.0583$, the nondimensional damping coefficient is $\zeta = 0.045$ and the effective length of the blade channels is $N_R = 0.285$ (No. of blade revolutions about the hub).

Numerical Simulation of Cavitating Flows

Hydrodynamics Bearings

This section describes the application of the isenthalpic two-phase flow model to the study of cavitation and ventilation effects in plane journal bearings with whirling eccentricity, as illustrated in Figure 4. A non-linear analysis that accounts for the inertia of the lubricant is used to determine the reaction forces caused by the shaft's eccentric motion both in the viscosity-dominated regime and at intermediate values of the Reynolds number, where the inertia of the lubricant is no longer negligible. The classical iteration method for the Reynolds lubrication equation (Muster and Sternlicht, 1965; Mori and Mori, 1991; Reinhardt and Lund, 1975) has been extended to the unsteady two-phase flow case in order to account for flow acceleration effects in the presence of cavitation and/or ventilation. Significant deviations from the steady-state case have been obtained at moderately high Reynolds numbers ($\mathrm{Re} = \omega RC/\nu_L \cong 10$).

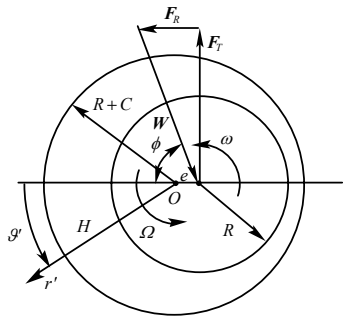

Figure 4. Schematic of the bearing configuration and forces.

In the coordinates r', ϑ', centered in O on the hub axis and rotating at the whirl speed Ω, the Reynolds equation for the flow in a plane journal bearing supporting a shaft of radius R, radial clearance C, rotational velocity ω and whirling eccentricity e (see Figure 4) becomes:

$$\frac{dp_0}{d\vartheta'} = -\frac{2\Lambda\dot{m}_0}{\rho\omega RH^3} + \frac{\Lambda\left(u_S + u_H\right)}{\omega RH^2} \qquad \text{and} \qquad \frac{d\dot{m}_0}{d\vartheta'} = 0$$

with periodic boundary conditions $p\left(\vartheta'\right) = p\left(\vartheta' + 2\pi\right)$ imposed to the pressure and (constant) mass flow in the bearing:

$$\dot{m}_0 = \int_R^{R+H} \rho u_0' \, dr' = -\frac{\rho H^3}{12\mu R}\frac{dp_0}{d\vartheta'} + \frac{\rho H}{2}\left(u_S' + u_H'\right)$$

In the above equations, $\Lambda = 6\mu\omega R^2$ is the bearing number, $u_H' = -\Omega\left(R + C\right)$ is the hub velocity and, to the first order in the eccentricity, the height of the lubricating film is $H \cong C + e\cos\vartheta'$, while the shaft velocity is $u_S' \cong \left(\omega - \Omega\right)R + \Omega e\cos\vartheta'$. In addition, in infinitely long bearings either the supply pressure of the lubricant, p_{inj}, is specified at some appropriate location ϑ_{inj}, or the overall void fraction of the fluid film is assigned:

$$\bar{\alpha} = \frac{1}{2\pi RC}\int_{\vartheta}^{\vartheta+2\pi} \alpha HR \, d\vartheta$$

In high power density turbomachines the increase of the shaft speed, possibly combined with the use of low-viscosity lubricants, can raise the modified Reynolds number $\mathrm{Re}^* = \omega C^2/\nu_L$ of the bearing significantly above unity. In this case the left hand side of the momentum equation for the lubricating fluid is no longer negligible. In the present work inertial effects have been included using the iteration method (Kahlert, 1947), assuming that they represent a small correction of the Reynolds solution and can be approximated using the velocity field, $\boldsymbol{u}_0$, p_0, obtained in the absence of inertial forces. Hence, the differential problem for the pressure field with inertial effects is:

$$\frac{dp_1}{d\vartheta'} = -\frac{2\Lambda\dot{m}_1}{\rho\omega RH^3} + \frac{\Lambda\left(u_S + u_H\right)}{\omega RH^2} + \rho_0\Psi_0 \quad \text{and} \quad \frac{d\dot{m}_1}{d\vartheta'} = 0$$

where $\dot{m}_1$ is the corrected mass flow rate across the lubricating film, and, after some lengthy algebra:

$$\Psi_0 = \left(\frac{2u_S - u_H}{10} - \frac{3}{140}\frac{H^2}{\mu R}\frac{dp_0}{d\vartheta'}\right)\omega\frac{dH}{d\vartheta'} + \frac{d}{d\vartheta'}\ln\left(\rho_0 H\right) \times \frac{1}{5}\left[u_S^2 + u_H^2 + 4u_S u_H - \frac{17}{28}\frac{\left(u_S + u_H\right)H^2}{\mu R}\frac{dp_0}{d\vartheta'} + \frac{3}{56}\left(\frac{H^2}{\mu R}\frac{dp_0}{d\vartheta'}\right)^2\right]$$

Table 1. Reference Bearing Parameters

Shaft radius	$R = 0.05$ m	Lubricant viscosity	$\mu_L = 0.0127$ Pa s
Relative clearance	$C/R = 2.9\cdot10^{-3}$	Modified Reynolds number	$\mathrm{Re}^* = \omega C^2/\nu_L = 0.08$
Relative eccentricity	$\varepsilon = e/C = 0.6$	Bearing number	$\Lambda = 0.009$ N
Shaft rotational speed	$\omega = 48.1$ rad/s	Gas mass fraction in the cavities	$X_g = 0.1$
Shaft whirl speed	$\Omega = 0$ rad/s	Alternative flow conditions:	
Lubricant temperature	$T_L = 70$ °C	average void fraction	$\bar{\alpha} = 0.154$
Lubricant saturation pressure	$p_{\text{sat}} \cong 35$ kPa	injection pressure @ $\vartheta_{\text{inj}}' = 0°$	$p_{\text{inj}} = 100$ kPa
Lubricant density	$\rho_L = 1000$ kg/m^3		

A single shooting method with fifth order Runge-Kutta integration and self-adaptive step size has been chosen to numerically integrate the two points boundary value problem for the bearing flow, with or without corrections for inertial effects depending on the value of the modified Reynolds number Re^*. A multidimensional Newton-Raphson method has been used to iterate on the unknown initial conditions until the end-point boundary conditions are met with the required accuracy. The convergence and speed of the method remain excellent, even though they appreciably deteriorate in flows with extensive cavitation and low vapor pressure, especially at high Reynolds numbers and relative eccentricities.

Unless stated otherwise, the results reported in the following refer to journal bearings whose main characteristic parameters are summarized in Table 1. The two-phase flow model and the numerical scheme for the prediction of cavitation in journal bearings have been successfully validated (Rapposelli and d'Agostino, 2001) against the experimental results by Floberg (1957a).

Let consider first the behavior of whirling and cavitating bearings with negligible inertia of the lubricant ($\mathrm{Re}^* << 1$). In this case the effect of the whirl speed on the nondimensional radial and tangential rotordynamic forces, F_R and F_T, normalized with $\pi\left(\Lambda/R\right)\left(R/C\right)^2$, is shown in Figure 5. In the absence of cavitation ($\bar{\alpha} = 0$) the computations predict

zero radial force and linearly-varying tangential force in accordance with known results for single-phase incompressible flows of constant vorticity (Vance 1988, Brennen 1994):

$$F_T = 2\varepsilon\left(\frac{1}{2} - \frac{\Omega}{\omega}\right)$$

At finite void fractions, both the radial and tangential forces deviate appreciably from these results and display a more complex dependence on the whirl speed. The presence of gas bubbles lowers the tangential force and generates a positive radial force, which increases rapidly with the void fraction and becomes comparable with the typical magnitude of the tangential force. The general features of the present solution at higher void fractions are consistent with the results of the π-approximation for cavitating bearings of low eccentricity (Vance 1988).

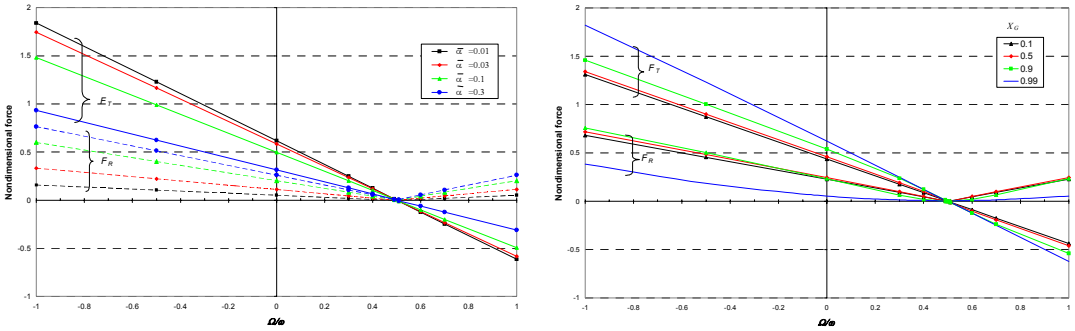

Figure 5. Radial and tangential rotordynamic forces, F_R (dashed lines) and F_T (solid lines), as functions of the whirl ratio Ω/ω for several values of the average void fraction $\bar{\alpha}$ and $\mathrm{Re}^* = 0.08$ (left) and several values of the mass fraction X_g of the noncondensable gas in the cavities with $\bar{\alpha} = 0.154$ (right).

It is worth recalling that rotordynamic forces are stabilizing when they tend to reduce the eccentricity and its whirl motion. Hence, with present notations and results, two-phase flow effects on the radial force are generally in favor of stability, but the tangential force remains destabilizing for whirl ratios Ω/ω ranging from 0 to about 0.5. In particular, consistently with the well-known features of the "oil whirl" instability (Newkirk and Taylor 1925, Hori 1959; Muszynska 1986), operation near $\Omega/\omega = 0.5$ is unstable because the eccentricity is not effectively controlled by the vanishing radial force and whirl motions can be sustained by the residual value of the tangential force. Notice that the extent of cavitation does not appreciably affect the "oil whirl" instability for $\Omega/\omega \cong 0.5$, but promotes stability for $0 < \Omega/\omega < 0.5$ by increasing the bearing stiffness and reducing the magnitude of the destabilizing tangential force.

In Figure 5 the combined effects of cavitation and ventilation on the rotordynamic forces are examined by varying the void fraction α (right) and the mass fraction X_g (left) of the noncondensable gas in the cavities. The results show that the radial force tends to assume a milder parabolic dependence on the whirl ratio near the whip frequency, while the tangential force remains nearly linear. The presence of appreciable concentrations of noncondensable gas in the lubricant also affects the magnitude of the rotordynamic forces. In particular, the tangential force increases monotonically with X_g, while the radial force slightly decreases near $\Omega/\omega \cong 0.5$ for $X_g < 0.9$ and then drops more significantly at all whirl ratios for X_g approaching the pure ventilation conditions ($X_g \cong 1$), when the pressure distribution becomes the more uniform as a consequence of the broader dispersion of the noncondensable gas throughout the lubricated annulus. Not surprisingly in view of earlier considerations, the occurrence of ventilated cavitation has therefore a significant destabilizing effect on the dynamics of the bearing.

Now consider the solution at moderate Reynolds numbers ($\mathrm{Re}^* > 1$). The influence of inertial effects on the bearing pressure distribution is illustrated in Figure 6 for some representative values of the whirl ratio. Except for the stationary case ($\Omega/\omega = 0$), comparison of the pressure profiles indicates that inertial effects significantly modify the pressure profile and the end point of the cavity, but have practically no influence on the inception location. The introduction of inertial effects reduces the bearing pressures at all whirl ratios but for the potentially unstable region $0 < \Omega/\omega < 0.5$ of the whirl spectrum, where the pressure profiles increase. Accordingly, for Reynolds numbers $\mathrm{Re}^* > 1$ the rotordynamic forces are higher than in the absence of inertial effects for $0 < \Omega/\omega < 0.5$, and smaller for the other whirl ratios, as illustrated in Figure 6. One can therefore conclude that for moderate Reynolds numbers ($\mathrm{Re}^* \cong 1 \approx 10$) inertial effects promote the rotordynamic stability of whirling and cavitating bearings. A second noteworthy aspect emerging from the above results is that even inertial effects that are practically undetectable in the stationary case ($\Omega/\omega = 0$) can

nevertheless become quite significant in whirling bearings, because the eccentric motion effectively enhances the magnitude of the inertial forces developing in the lubricant.

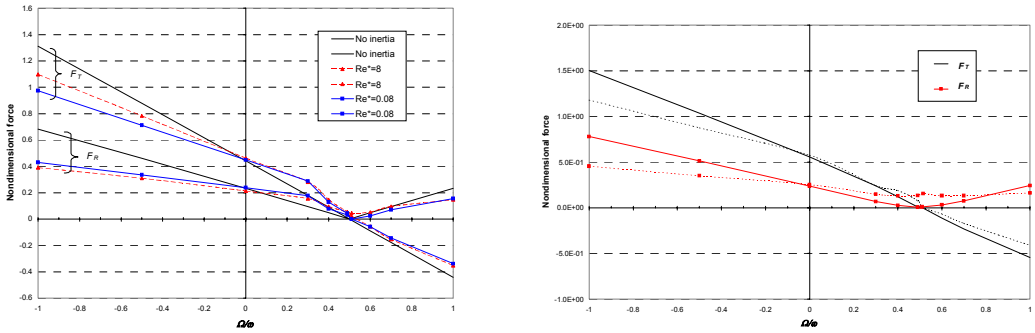

Figure 6. Radial and tangential rotordynamic forces, F_R and F_T, as functions of the whirl ratio Ω/ω in a whirling bearing with inertial effects (dots) and without inertial effects (solid lines). The modified Reynolds numbers are $\mathrm{Re}^* = 0.08$ and 8. On the right side rotordynamic forces at an increased value of the relative clearance $C/R = 0.03$, for a modified Reynolds numbers $\mathrm{Re}^* = 0.08$.

Finally, we briefly examine the effects of increasing the relative clearance, a situation that can be practically relevant in connection with the response of squeezed-film dampers. The behavior of the rotordynamic forces at a tenfold higher value of the relative clearance ($C/R = 0.03$) is shown in Figure 6 (right side) as a function of the whirl ratio Ω/ω. As expected, the introduction of inertial effects effectively stabilizes the bearing motion by inducing significant positive component of the radial force for positive whirl, and in particular near the unstable whip speed $\Omega/\omega \cong 0.5$. On the other hand, the remaining frequencies of the frequency spectrum the impact of inertial effects remains qualitatively unchanged even at high clearances.

Hydrofoils and Headforms

In this area of research Centrospazio has collaborated with CIRA (Centro Italiano Ricerche Aerospaziali) to the development of the two-phase flow model and the numerical code for simulating steady and unsteady cavitating flows in 2D configurations, both planar (hydrofoil) and axisymmetric (headforms). The simulation of cavitating flow requires the application of specialized methods because usual numerical schemes developed for compressible or incompressible flows are not capable of handling in a unified manner the simultaneous presence of extremely compressible cavitation pockets and practically incompressible fully-wetted flow regions separated by very rapid shock-like transitions. In view of these considerations, a pressure-based method based on the SIMPLE (Semi-Implict Method for Pressure-Linked Equations) algorithm has been chosen. With finite volume discretization in conservative form and Karki's compressibility correction, the method is shock-capturing and stable over a wide range of subsonic and supersonic Mach numbers, and has been tested with quite encouraging success in the analysis of cavitating flows in 2D axisymmetric and planar flow configurations (d'Agostino et al. 2001; Salvatore, Pascarella & d'Agostino, 2001).

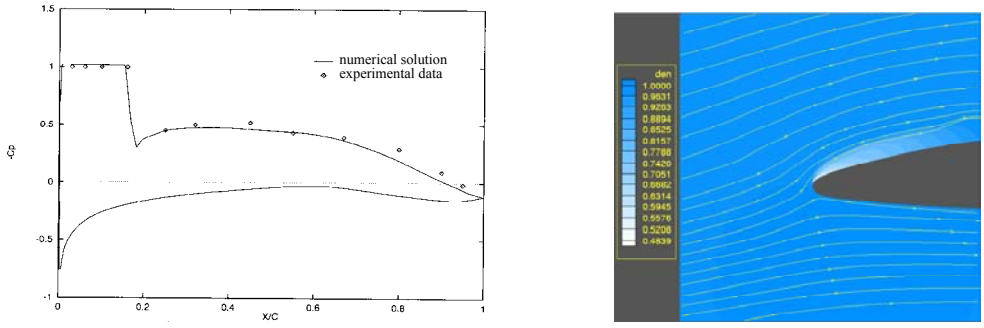

Figure 7. Comparison of the computed surface pressure coefficient (solid line) with the experimental data by Shen and Dimotakis, 1984 (dots), nondimensional density distribution ρ/ρ_L and streamline map for developed cavitation in water on the modified NACA 66-109 hydrofoil. The flow conditions are: $\sigma = 1$, $T_L = 20°\mathrm{C}$, $\vartheta = 4°$ (angle of attack) and $\mathrm{Re}_c = 2 \cdot 10^6$.

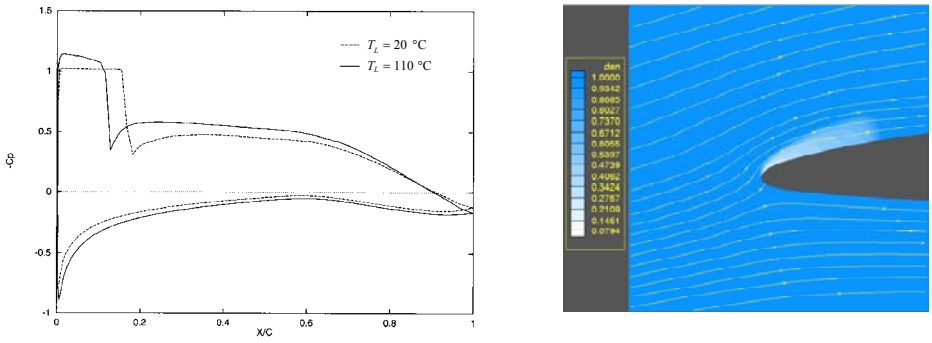

Figure 8. Comparison of the computed surface pressure coefficient, nondimensional density distribution ρ/ρ_L and streamline map for incipient cavitation in water on the modified NACA 66-109 hydrofoil at $T_L = 20$ °C (dotted line) and $T_L = 100$ °C (solid line). The flow conditions are: $\sigma = 1$, $\vartheta = 4°$ (angle of attack) and $\mathrm{Re}_c = 2 \cdot 10^6$.

An example of the surface pressure distribution and the density map for incipient cavitation ($\sigma = 1$) on the modified NACA 66-109 hydrofoil at 4° incidence and $\mathrm{Re} = u_\infty c/\nu_L = 2 \cdot 10^6$ are presented in Figure 7. The simulations are in satisfactory agreement with the measured data by Shen and Dimotakis (1989) both in terms of the location and length of the cavitation region and the shape of the surface pressure profile. A sharp suction peak occurs at the leading edge, originating the formation of a cavitation region with practically constant pressure. The effect of increasing the temperature of the flow from 20 °C to 100 °C is illustrated in Figure 8. In the lack of reference experimental data, the quantitative assessment of thermal cavitation effects is hampered by the uncertain dependence of the parameter δ_T/R with the flow temperature. Comparison of Figures 7 and 8 indicates that at elevated temperatures:

- cavitation occurs for σ significantly smaller than $-C_{p\min}$ (thermal scaling);
- the length of the cavitation region decreases appreciably;
- the pressure in the cavitation region becomes less uniform and increases in the streamwise direction.

These findings are fully consistent with the limited available experimental evidence.

Conclusions and Future Work

The results of recent work on cavitation modeling and simulation at Centrospazio confirm that the main features of thermal effects in cavitating flows can indeed be captured by the proposed model with proper choice of δ_T/R. Further experience with the application of the model to flows with well documented thermal cavitation effects is needed in order to obtain reliable estimates of δ_T/R in water and the other technical fluids of interest for accurate simulation of cavitating flows in rocket propulsion applications. To this purpose current numerical activities at Centrospazio and the Dipartimento di Ingegneria Aerospaziale, Università degli Studi di Pisa, are now geared toward the in-house development of a 3D, density-based, implicit, preconditioned code, which employs the above cavitation model on unstructured grids, optimized for flow analyses in the complex geometries typical of rocket propellant feed turbopumps. At the same time Centrospazio is also actively involved in experimental work on turbopump cavitation with thermal effects, whose results will contribute to provide useful data for supporting ongoing modeling and simulation activities.

More generally, recent work carried out at Centrospazio on the fluid dynamics of two-phase and cavitating flows in turbopumps for space applications found favorable acceptance in the scientific community and places Centrospazio in an advantageous position for usefully contributing to technical progress in this field.

Acknowledgements

The present work has been supported by the Agenzia Spaziale Italiana under the 1997 - 2000 contracts for fundamental research. The authors would like to acknowledge the help Mr. Roberto Merlo, Mr. Roberto Falorni, and Mr. Marco-Rosario Venturini-Autieri and express their gratitude to Profs. Mariano Andrenucci and Renzo Lazzeretti of the Dipartimento di Ingegneria Aerospaziale, Università degli Studi di Pisa, Pisa, Italy, for their constant and friendly encouragement.

References

Bhattacharyya A., 1994, "Internal Flows and Force Matrices in Axial Flow Inducers", *Ph. D. thesis, Div. Eng. & Appl. Science, Caltech*, Pasadena, CA, USA.

Braisted D.M. & Brennen C.E., 1980, "Auto-oscillation of Cavitating Inducers", *Polyphase Flow and Transport Technology, ed. R.A. Bajura,* ASME Publ., New York, pp. 157-166.

Brennen C.E., 1994, "Hydrodynamics of Pumps", *Concepts ETI, Inc*. and *Oxford University Press*.

Brennen C. E., 1995, "Cavitation and Bubble Dynamics", *Oxford University Press*.

Brennen C.E. & Acosta A.J., 1976, "The Dynamic Transfer Function for a Cavitating Inducer", *ASME J. Fluids Eng*., Vol. 98, pp. 182-191.

Brennen C.E. & Acosta A.J., 1973, "Theoretical, Quasi-Static Analysis of Cavitation Compliance in Turbopumps", *J. Spacecrafts & Rockets*, Vol. 10, No. 3, pp. 175-180.

d'Agostino L. & d'Auria F., 1997, "Three-Dimensional Analysis of Rotordynamic Forces on Whirling and Cavitating Inducers", *ASME FED Summer Meeting*, Vancouver, BC, Canada, June 22-26.

d'Agostino L., d'Auria F. & Brennen C.E., 1998, "A Three-Dimensional Analysis of Rotordynamic Forces on Whirling and Cavitating Helical Inducers", *ASME J. of Fluids Eng.,* Vol. 120, pp. 698-704.

d'Agostino L., Rapposelli E., Pascarella C. & Ciucci A., 2001, "A Modified Bubbly Isenthalpic Model for Numerical Simulation of Cavitating Flows", AIAA Paper 2001-3402, *37th AIAA/ASME/SAE/ASEE Joint Propulsion Conference*, Salt Lake City, Utah, USA, July 8-11.

d'Agostino L., & Venturini-Autieri M., 2002, "Three-Dimensional Analysis of Rotordynamic Fluid Forces on Whirling and Cavitating Finite-Length Inducers", *9th Int. Symp. on Transport Phenomena and Dynamics of Rotating Machinery (ISROMAC-9),* Honolulu, HI, USA, February 10-14.

d'Auria F., d'Agostino L. & Brennen C.E., 1994, "Linearized Dynamics of Bubbly and Cavitating Flows in Cylindrical Ducts", *ASME FED Summer Meeting, Incline Village*, NV, USA, June 19-23.

d'Auria F., d'Agostino L. & Brennen C.E., 1995, "Bubble Dynamic Effects on the Rotordynamic Forces in Cavitating Inducers", *ASME FED Summer Meeting*, Hilton Island, SC, USA, August 13-18.

Dowson, D., Taylor, C.M., 1975, "Fundamental Aspects of Cavitation in Bearings", *1st Leeds-Lyon Int. Symp. on Trib*., pp. 15-26.

Floberg L., 1957, *Trans. Chalmers Univ. of Technology*, Vol. 189, Götheburg, Sweden.

Franz R. et al., 1989, "The Rotordynamic Forces on a Centrifugal Pump Impeller in the Presence of Cavitation", *ASME FED-81*, pp. 205-212.

Goirand B., Mertz A.L., Jousselin F. & Rebattet C., 1992, "Experimental Investigations of Radial Loads Induced by Partial Cavitation with Liquid Hydrogen Inducer", *IMechE, C453/056*, pp. 263-269.

Jery B. et al., 1985, "Forces on Centrifugal Pump Impellers", *2nd Int. Pump Symp*., Houston, TX, USA, April 29-May 2, 1985.

Hori Y., 1959, "The Theory of Oil Whip", *ASME J. Appl. Mech*., Vol. 26, pp. 189-198.

Kahlert W., 1947, *Ingr.Archiv*, Vol. 16, pp. 321-342.

Kamijo K., Yoshida M. & Tsujimoto Y., 1993, "Hydraulic and Mechanical Performance of LE-7 LOX Pump Inducer", *ASME J. Propulsion and Power*, Vol. 9, No. 6, pp. 819-826.

Mori A. & Mori H., 1991, "Re-Examination of Film Rupture Boundary Condition in Hydrodinamic Lubrication under Inertia Effect", *ASME J. of Tribology*, Vol. 113, pp. 604-608.

Muster D. & Sternlicht B., ed., 1965, *Proc. Int. Symp. on Lubrication and Wear*.

Muszynska A., 1986, "Whirl and Whip Rotor/Bearing Stability Problems", *J. Sound and Vibrations*, Vol. 110, pp. 443-463.

NASDA, 2000a, *Report No. 94*, May 2000.

NASDA, 2000b, *Report No. 96*, June 2000.

Natanzon M.S. et al., 1974, "Experimental Investigation of Cavitation Induced Oscillations of Helical Inducers", *Fluid Mech. Soviet Res*., Vol. 3 No. 1, pp.38-45.

Ng S.L. & Brennen C.E., 1978, "Experiments on the Dynamic Behavior of Cavitating Pumps", *ASME J. Fluids Eng*., Vol. 100, No. 2, pp. 166-176.

Newkirk B.L. and Taylor H.D., 1925, "Shaft Whipping due to Oil Action in Journal Bearing", *General Electric Review*, August, pp. 559-568.

Rapposelli E. & d'Agostino L., 2001, "A Modified Isenthalpic Model of Cavitation in Plane Journal Bearings", *CAV2001, International Symposium on Cavitation*, Pasadena, California USA, June 20-23.

Rapposelli E., Falorni R. & d'Agostino L., 2002, "Two-Phase and Inertial Effects on the Rotordynamic Forces in Whirling Journal Bearings", *Proc. 2002 ASME FED Summer Meeting*, Montreal, Quebec, Canada, July 14-18.

Reinhardt E. & Lund J.W., 1975, "The Influence of Fluid Inertia on the Dynamic Properties of Journal Bearings", *ASME J. Lubrication Technology*, Vol. 97, Sez. F, pp. 159-167.

Rosenmann W., 1965, "Experimental Investigations of Hydrodynamically Induced Shaft Forces with a Three Bladed Inducer", *Proc. ASME Symp. on Cavitation in Fluid Machinery*, pp. 172-195.

Rubin S., 1966, "Longitudinal Instability of Liquid Rockets due to Propulsion Feedback (POGO)", *J. of Spacecraft and Rockets*, Vol.3, No. 8, pp.1188-1195.

Ryan R.S., Gross L.A., Mills D. & Michell P., 1994, "The Space Shuttle Main Engine Liquid Oxygen Pump High-Synchronous Vibration Issue, the Problem, the Resolution Approach, the Solution", *AIAA Paper 94-3153*.

Sack L.E. & Nottage H.B., 1965, "System Oscillations Associated to Cavitating Inducers", *ASME J. Basic Eng*., Vol. 87, pp. 917-924.

Salvatore V., Pascarella C. & d'Agostino L., 2001, "Numerical Evaluation of Cavitating Flows Using Different Two-Phase Models", ICMF2001 Paper 713, New Orleans, Luoisiana USA, June.

Shen Y.T. & Dimotakis P.E., 1989, "The Influence of Surface Cavitation on Hydrodynamic Forces", Proc. 22nd ATTC, St. Johns

Stripling L.B. & Acosta A.J., 1962, "Cavitation in Turbopumps – Part 1, *ASME J. Basic Eng*., Vol. 84, pp. 326-338.

Swales P.D., 1975, "A Review of Cavitation Phenomena In Engineering Situations", *1st Leeds-Lyon Int. Symp. on Trib*., pp. 3-9.

Vance J.M., 1988, "Rotordynamics of Turbomachinery", *John Wiley and Sons*, New York, USA.

Zoladz T., 2002, *personal communication*.